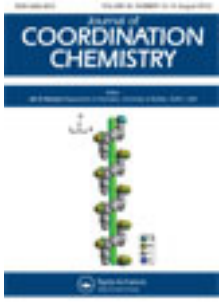

Journal of Coordination Chemistry
Publication details, including instructions for authors and subscription information:
http://www.tandfonline.com/loi/gcoo20

A zinc(II) complex with tris(2-(N-methyl)benzimidazlylmethyl)amine and salicylate: synthesis, crystal structure, and DNA-binding

Huilu Wu [a], Ying Bai [a], Jingkun Yuan [a], Hua Wang [a], Guolong Pan [a], Xuyang Fan [a] & Jin Kong [a]

[a] School of Chemical and Biological Engineering, Lanzhou Jiaotong University, Lanzhou 730070, P.R. China

Accepted author version posted online: 27 Jun 2012.Published online: 06 Jul 2012.

To cite this article: Huilu Wu, Ying Bai, Jingkun Yuan, Hua Wang, Guolong Pan, Xuyang Fan & Jin Kong (2012) A zinc(II) complex with tris(2-(N-methyl)benzimidazlylmethyl)amine and salicylate: synthesis, crystal structure, and DNA-binding, Journal of Coordination Chemistry, 65:16, 2839-2851, DOI: 10.1080/00958972.2012.707314

To link to this article: http://dx.doi.org/10.1080/00958972.2012.707314

Journal of Coordination Chemistry
Vol. 65, No. 16, 20 August 2012, 2839–2851

A zinc(II) complex with tris(2-(*N*-methyl)benzimidazlylmethyl) amine and salicylate: synthesis, crystal structure, and DNA-binding

HUILU WU*, YING BAI, JINGKUN YUAN, HUA WANG, GUOLONG PAN, XUYANG FAN and JIN KONG

School of Chemical and Biological Engineering, Lanzhou Jiaotong University, Lanzhou 730070, P.R. China

(*Received 26 January 2012; in final form 14 May 2012*)

A five-coordinate zinc complex with tris(2-(*N*-methyl)benzimidazylmethyl)amine (Mentb) and salicylate, with composition [Zn(Mentb)(salicylate)](NO_3), was synthesized and characterized by elemental analysis, IR and UV-Vis spectral measurements. The crystal structure of the zinc complex shows that Zn(II) is bonded to tris(2-(*N*-methyl)benzimidazylmethyl)amine (Mentb) and a salicylate through four nitrogens and one oxygen, and the coordination geometry is best described as distorted trigonal-bipyramid. The DNA-binding of the Zn(II) complex and Mentb were investigated by spectrophotometric methods and viscosity measurements, and the results suggest that the Zn(II) complex binds to DNA *via* intercalation; the binding affinity of the Zn(II) complex to DNA is greater than Mentb. Additionally, Zn(II) complex exhibited potential to scavenge hydroxyl radical *in vitro*.

Keywords: Tris(2-(*N*-methyl)benzimidazlylmethyl)amine; Crystal structure; Zinc(II) complex; DNA-Binding properties

1. Introduction

Benzimidazole is a heterocycle with a nitrogen donor and is a component of biologically important molecules [1]; its derivatives and their metal complexes have been extensively investigated [2–4]. The tetradentate tripodal, tris(2-(N-methyl)benzimidazlylmethyl) amine (Mentb), is similar to benzimidazole in its mode of coordination [5]. Since the three arms of this type of ligand can each rotate freely around a N(apical)–C bond, multicomponent complexes or coordination polymeric networks may be expected to form with metal ions of low coordination number. We have been interested in the coordinating ability of benzimidazolic ligands toward transition metal ions [6–9].

Benzimidazole as a ligand toward transition metal ions has been of interest for design and synthesis of DNA cleaving reagents in a number of biological models [10–14]. Low molecular weight metal complexes are attractive mimics because of their diverse electronic structures [15]; such studies can help us understand and clarify the role of

*Corresponding author. Email: wuhuilu@163.com

ISSN 0095-8972 print/ISSN 1029-0389 online
http://dx.doi.org/10.1080/00958972.2012.707314

metal ions in natural nucleases. Transition metal complexes can interact with DNA through three non-covalent modes: intercalation, groove binding, and external static electronic effects [16, 17]. Among these interactions, intercalation is the most important one because small molecules binding to DNA *via* intercalation often possess potential anticancer activities. The search for drugs binding to DNA *via* intercalation has been a focus [18, 19]. Zn is an ideal agent to mediate cleavage of phosphate diester backbone due to its redox inertness and hard Lewis acid properties [20].

Herein, we have prepared and investigated the properties and crystal structure of the Zn(II) complex with the tripod tris(2-(*N*-methyl)benzimidazylmethyl)amine (Mentb). Moreover, we describe a comparative study of the interaction of the ligand and its complex with calf thymus DNA using electronic absorption and viscosity measurement.

2. Experimental

2.1. *Materials and physical measurement*

All chemicals were of analytical grade. Ethidium bromide (EB) and calf thymus DNA (CT-DNA) were purchased from Sigma and used without purification. All experiments involving interaction of the ligand and the complex with CT-DNA were carried out in doubly-distilled water buffer containing 5 mM Tris and 50 mM NaCl adjusted to pH 7.2 with hydrochloric acid. A solution of CT-DNA gave a ratio of UV absorbance at 260 and 280 nm of about 1.8–1.9, indicating that the CT-DNA was sufficiently free of protein [21]. The CT-DNA concentration per nucleotide was determined spectrophotometrically by employing an extinction coefficient of 6600 $(\text{mol L}^{-1})^{-1}\,\text{cm}^{-1}$ at 260 nm [22].

C, H, and N elemental analyses were determined using a Carlo Erba 1106 elemental analyzer. IR spectra were recorded from 4000–400 cm^{-1} with a Nicolet FT-VERTEX 70 spectrometer using KBr pellets. Electronic spectra were taken on Lab-Tech UV Bluestar and Spectrumlab 722sp spectrophotometers and the spectral resolution used is 0.2 nm. Fluorescence spectra were recorded on a LS-45 spectrofluorophotometer.

2.2. *DNA-binding study*

Absorption titration experiments were performed with fixed concentrations of complex and ligand, while gradually increasing the concentration of CT-DNA. To obtain the absorption spectra, the required amount of CT-DNA was added to the compounds and reference solutions in order to eliminate the absorbance of CT-DNA itself. From the absorption titration data, the binding constant (K_b) was determined using equation [23]:

$$[\text{DNA}]/(\varepsilon_a - \varepsilon_f) = [\text{DNA}]/(\varepsilon_b - \varepsilon_f) + 1/K_b(\varepsilon_b - \varepsilon_f)$$

where [DNA] is the concentration of CT-DNA in base pairs, ε_a corresponds to the observed extinction coefficient (Aobsd/[M]), ε_f corresponds to the extinction coefficient of the free compound, ε_b is the extinction coefficient of the compound when fully bound to CT-DNA, and K_b is the intrinsic binding constant. The ratio of slope to intercept in the plot of $[\text{DNA}]/(\varepsilon_a - \varepsilon_f)$ *versus* [DNA] gave the value of K_b.

Enhanced fluorescence of EB in the presence of DNA can be quenched by addition of a second molecule [24, 25]. The extent of fluorescence quenching of EB bound to CT-DNA can be used to determine the extent of binding between the second molecule and CT-DNA. Competitive binding experiments were carried out in the buffer by keeping [DNA]/[EB] = 1 and varying the concentrations of the compounds. The fluorescence spectra of EB were measured using an excitation wavelength of 520 nm, and the emission range was set between 550 and 750 nm. The spectra were analyzed according to the classical Stern–Volmer equation [26]:

$$I_0/I = 1 + K_{SV}[Q]$$

where I_0 and I are the fluorescence intensities at 599 nm in the absence and presence of the quencher, respectively, K_{sv} is the linear Stern–Volmer quenching constant, and [Q] is the concentration of the quencher. In these experiments [CT-DNA] = 2.5×10^{-3} mol L^{-1}, [EB] = 2.2×10^{-3} mol L^{-1}.

Viscosity experiments were conducted on an Ubbelodhe viscometer, immersed in a water bath maintained at 25.0 ± 0.1°C. Titrations were performed for the complexes (3–30 μM) and each compound was introduced into CT-DNA solution (42.5 μM) present in the viscometer. Data were analyzed as $(\eta/\eta_0)^{1/3}$ *versus* the ratio of the concentration of the compound to CT-DNA, where η is the viscosity of CT-DNA in the presence of the compound and η_0 is the viscosity of CT-DNA alone. Viscosity values were calculated from the observed flow time of CT-DNA-containing solutions corrected from the flow time of buffer alone (t_0), $\eta = (t - t_0)$ [27].

2.3. *Hydroxyl radical scavenger measurements*

Hydroxyl radicals were generated in aqueous media through the Fenton-type reaction [28, 29]. The reaction mixture (3 mL) contained 1.0 mL of 0.10 mmol aqueous safranin, 1 mL of 1.0 mmol aqueous EDTA–Fe(II), 1 mL of 3% aqueous H_2O_2, and a series of quantitative microadditions of solutions of the test compound. A sample without the tested compound was used as the control. The reaction mixtures were incubated at 37°C for 30 min in a water bath. The absorbance was then measured at 520 nm. All the tests were run in triplicate and are expressed as the mean and standard deviation [30]. The scavenging effect for OH· was calculated from the following expression:

$$\text{Scavenging ratio (\%)} = [(A_i - A_0)/(A_c - A_0)] \times 100\%$$

where A_i = absorbance in the presence of the test compound, A_0 = absorbance of the blank in the absence of the test compound, and A_c = absorbance in the absence of the test compound, EDTA-Fe(II) and H_2O_2.

2.4. *Preparation of the ligand and its complex*

2.4.1. Preparation of tris(2-(N-methyl)benzimidazlylmethyl)amine (Mentb). Mentb was synthesized by the literature method [31]. Yield: 4.6 g (51%); m.p.: 215–217°C. Calcd (%) for $C_{27}H_{27}N_7$: C, 72.14; H, 6.05; N, 21.81. Found (%): C, 72.27; H, 6.17; N, 21.73. UV-Vis (λ, nm): 279, 289. FT–IR (KBr ν/cm^{-1}): 1288 ν(C–N); 1477 ν(C=N); 1614 ν(C=C).

2.4.2. Preparation of complex. To a stirred solution of Mentb (0.449 g, 1 mmol) in hot MeOH (10 mL) was added $Zn(NO_3)_2 \cdot 6H_2O$ (0.297 g, 1 mmol) in MeOH (5 mL), and salicylate (0.160 g, 1 mmol) in hot MeOH (5 mL), sequentially. A white product formed rapidly, was filtered off, washed with MeOH and absolute Et_2O, and dried *in vacuo*. The dried precipitate was dissolved in DMF to form a colorless solution into which Et_2O was allowed to diffuse at room temperature. White crystals suitable for X-ray measurement were obtained after three weeks. Yield: 0.46 g (51%). Calcd (%) for $C_{34}H_{32}ZnN_8O_6$: C, 57.19; H, 4.52; N, 15.69. Found (%): C, 57.10; H, 4.48; N, 15.52. UV-Vis (λ, nm): 280, 297. FT–IR (KBr ν/cm^{-1}): 1239 ν(C–N); 1484 ν(C=N); 1622 ν(C=C); 1579 ν_{as}(O–C–O); 1396 ν_s(O–C–O); 1393 ν(N–O).

2.5. *X-ray crystallography*

A suitable single crystal was mounted on a glass fiber and the intensity data were collected on a Bruker Smart CCD diffractometer with graphite-monochromated Mo-Kα radiation (λ = 0.71073 Å) at 296 K. Data reduction and cell refinement were performed using the SMART and SAINT programs [32]. The structure was solved by direct methods and refined by full-matrix least squares against F^2 using SHELXTL software [33]. All hydrogen atoms were found in difference electron maps and were subsequently refined in a riding-model approximation with C–H distances ranging from 0.93 to 0.97 Å and $U_{iso}(H) = 1.2U_{eq}(C)$ and $U_{iso}(H) = 1.5U_{eq}(C_{methyl})$. Basic crystal data, description of the diffraction experiment, and details of the structure refinement are given in table 1. Selected atomic distances and bond angles of

Table 1. Crystal data and structure refinement for [Zn(Mentb)(salicylate)](NO_3).

Molecular formula	$C_{34}H_{32}ZnN_8O_6$
Molecular weight	714.07
Crystal system	Triclinic
Space group	$P\bar{1}$
Unit cell dimensions (Å, °)	
a	10.756(4)
b	14.287(5)
c	14.816(6)
α	109.619(4)
β	103.796(4)
γ	105.582(4)
Volume (Å^3), *Z*	1925.5(13), 1
Calculated density (g cm^{-3})	1.232
F (000)	740
Crystal size (mm^3)	0.38 × 0.32 × 0.30
θ range for data collection (°)	2.12–25.50
Limiting indices	$-13 \le h \le 13$; $-17 \le k \le 17$; $-17 \le l \le 17$
Reflections collected	12,429
Independent reflections	6991 [R(int) = 0.0520]
Refinement method	Full-matrix least-squares on F^2
Data/restraints/parameters	6991/0/446
Goodness-of-fit on F^2	0.878
Final *R* indices [$I > 2\sigma(I)$]	$R_1 = 0.0598$, $wR_2 = 0.1237$
R indices (all data)	$R_1 = 0.1266$, $wR_2 = 0.1421$

[Zn(Mentb)(salicylate)](NO_3) are listed in table 2. The intramolecular O···H···O hydrogen bond in the complex [Zn(Mentb)(salicylate)](NO_3) are listed in table 3.

3. Results and discussion

The Zn(II) complex is soluble in DMF and DMSO, but insoluble in water and other organic solvents, such as methanol, ethanol, benzene, petroleum ether, trichloromethane, etc. The elemental analyses show that its composition is [Zn(Mentb)(salicylate)](NO_3).

3.1. *IR and electronic spectra*

In free Mentb, a strong band at 1477 cm^{-1} with a weak band at 1516 cm^{-1} are observed. By analogy with the assigned bands of imidazole, the former can be attributed to (C=N–C=C), while the latter can be attributed to (C=N) [34, 35]. Two bands are found at 1485 and 1502 cm^{-1} of the complex, shifted 8–14 cm^{-1}, which implies direct coordination of all four imine nitrogen atoms to Zn(II). This is the preferred

Table 2. Selected atomic distances (Å) and angles (°) for the Zn(II) complex.

Bond distances			
Zn–N1	2.413(3)	Zn–N3	2.055(4)
Zn–N5	2.046(3)	Zn–N7	2.076(3)
Zn–O1	1.982(3)		
Bond angles			
N5–Zn–N3	110.94(14)	N5–Zn–N7	113.55(13)
N3–Zn–N7	114.69(13)	N3–Zn–O1	110.73(13)
N5–Zn–O1	111.74(14)	N7–Zn–O1	94.16(14)
N5–Zn–N1	74.81(13)	N3–Zn–N1	74.46(13)
O1–Zn–N1	168.12(12)	N7–Zn–N1	74.00(13)

Table 3. Hydrogen bonds for $[Zn(Mentb)(salicylate)]^+$ (Å and °).

D–H···A	*d*(D–H)	*d*(H···A)	*d*(D···A)	∠(DHA)
C(1)–H(1A)···O(3)#2	0.97	2.51	3.342(6)	144
O(3)–H(3)···O(2)#1	0.82	1.80	2.525(5)	146
C(3)–H(3C)···O(6)#1	0.96	2.47	3.217(8)	134
C(8)–H(8)···O(2)#1	0.93	2.31	3.161(7)	152
C(10)–H(10A)···O(6)#1	0.97	2.58	3.388(7)	141
C(26)–H(26)···O(1)#1	0.93	2.59	3.216(6)	125
C(12)–H(12A)···O(4)#3	0.96	2.52	3.109(8)	120
C(19)–H(19A)···O(4)#3	0.97	2.52	3.416(8)	154
C(21)–H(21C)···O(5)#3	0.96	2.53	3.462(8)	165
C(12)–H(12B)···O(2)#4	0.96	2.34	3.233(6)	154
C(16)–H(16)···O(5)#4	0.93	2.54	3.268(7)	135

Symmetry transformations used to generate equivalent atoms: #1 x, y, z; #2 $x-1, y, z$; #3 $-x+1, -y+1, -z$; #4 $-x+2, -y+1, -z$.

coordination as found for other metal complexes with benzimidazoles [36]. Since the carboxylate can coordinate to metal bidentate or monodentate, the "Δ criterion", which is based on the difference between the ν_{as}(O–C–O) and ν_s(O–C–O) values, compared to the corresponding value in sodium carboxylate, determines the coordination of carboxylate [37–39]. IR spectral data of the complex show bands at 1579 and 1396 cm^{-1} ($\Delta\nu$ is 183 cm^{-1}), attributed to ν_{as}(O–C–O) and ν_s(O–C–O), implying monodentate carboxylate of salicylate [40]. Bands at 1393, 881, and 748 cm^{-1} indicate that nitrate (D_{3h}) is present [40].

DMF solutions of the ligand and its complex show, as expected, almost identical UV spectra. UV bands of Mentb (279 and 289 nm) are only marginally blue-shifted (8 nm) compared with the complex, evidence of C=N coordination to metal [41]. These bands are assigned to $\pi \rightarrow \pi^*$ (imidazole) transitions.

3.2. *X-ray structures of [Zn(Mentb)(salicylate)](NO$_3$)*

The molecular structure of the zinc(II) complex is shown in figure 1, consisting of $[Zn(Mentb)(salicylate)]^+$ and nitrate. The Zn(II) is five-coordinate with a ZnN_4O chromophore. Mentb is tetradentate and carboxylate of salicylate completes the coordination. The coordination geometry of Zn(II) is best described as distorted trigonal-bipyramid ($\tau = 0.89$), with approximate molecular symmetry C_3. The parameter τ is defined as $(\beta–\alpha)/60$ [where β = O1–Zn–N1, α = O3–Zn–N7] and its value varies from 0 (in a regular square-based pyramid) to 1 (in a regular trigonal bipyramid) [42]. The coordination geometry around Zn(II) appears to relieve the steric crowding. The equatorial plane is occupied by N3, N5, and N7 from three benzimidazolyl groups, while Zn(II) protrudes toward O1 and is 2.497 Å from the equatorial plane. Axial positions are occupied by N1 and O1, with Zn–N1 2.413(3) Å, Zn–O1 1.982(3) Å, and N1–Zn–O1 is 168.12(12)°. The bond distance between the zinc and the apical nitrogen is 2.413(3) Å, which is about 0.357 Å longer than the bond distances between the zinc ion and the trigonal basal nitrogen atoms (2.046, 2.055, and 2.067 Å, average 2.056 Å). The three benzimidazole ring arms of Mentb form a cone-shaped cavity. The angles of N3–Zn–N5, N3–Zn–N7, and N5–Zn–N7 are 110.94(14), 114.69(13), and 113.55(13)°, respectively. The N1–Zn–N3 [74.46(13)°], N1–Zn–N5 [74.81(13)°] and N1–Zn–N7 [74.00(13)°] angles, which are all *ca* 16° less than the ideal 90°, are imposed by the geometry of Mentb. The distance between Zn(II) and O2 is 3.038 Å, so O2 is not coordinated.

3.3. *DNA binding mode and affinity*

3.3.1. Electronic absorption. Electronic absorption spectroscopy has been widely employed to determine the binding characteristics of metal complexes with DNA [43–45]. We have investigated the binding mode of DNA with ligand and complex through absorption titration experiments. The absorption spectra of the free ligand and complex in the absence and presence of CT-DNA (at a constant concentration of complex) are given in figure 2. With increasing DNA concentrations, the hypochromisms are 30.92% at 279 nm for free Mentb; 43.74% at 280 nm for the complex. The λ_{max} for free Mentb increased from 279 to 282, while that for the complex increased

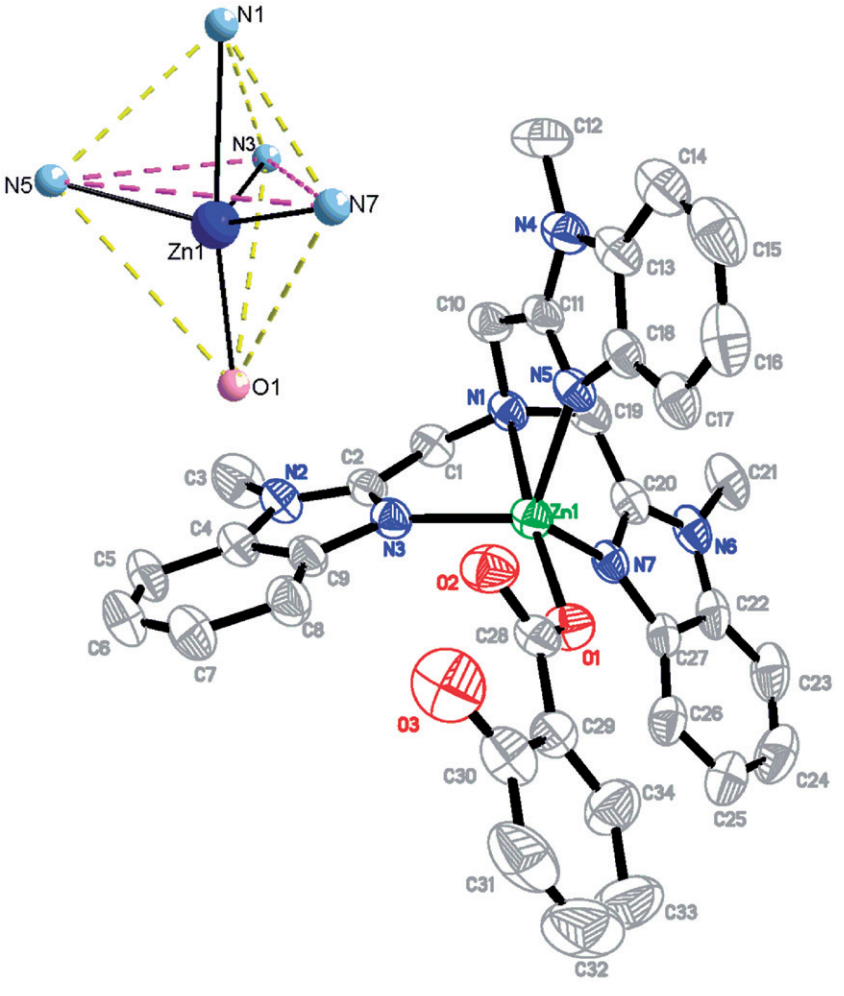

Figure 1. Molecular structure and atom numberings of $[Zn(Mentb)(salicylate)]^+$ with hydrogen atoms and nitrate omitted for clarity.

from 280 to 281 nm with slight red shifts of about ~1–3 nm under identical experimental conditions. The hypochromism suggests that the compounds interact with CT-DNA [46]. The K_b values of Mentb and complex were $3.28 \times 10^3 (\text{mol L}^{-1})^{-1}$ ($R = 0.99$ for 11 points) and $3.72 \times 10^4 (\text{mol L}^{-1})^{-1}$ ($R = 0.99$ for 16 points), respectively. Hence, the binding strength of complex is greater than the free ligand. This conclusion is similar with our previous research and the title complex is also stronger than those complexes [47].

The affinity for DNA is strong for Zn(II) complex when compared with the ligands. We attributed this difference to three possible reasons: (i) Charge transfer of coordinated Mentb, caused by coordination of Zn(II), results in reduction of charge density of the planar conjugate system. Therefore, this change will inevitably allow complexes to bind to DNA more easily [48]. (ii) This difference in their DNA binding ability also could be attributed to the presence of an electron deficient center in the

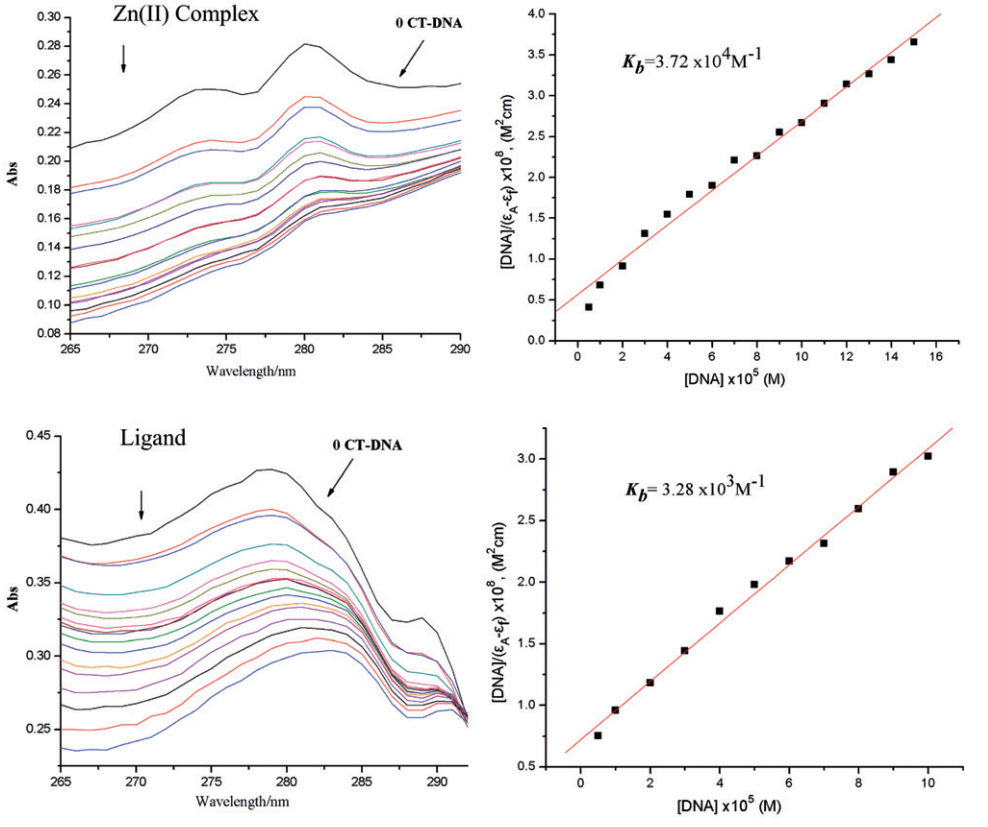

Figure 2. Electronic spectra of complex and ligand in Tris–HCl buffer upon addition of CT-DNA. [Compound] = 3×10^{-5} (mol L^{-1})$^{-1}$, [DNA] = 2.5×10^{-5} (mol L^{-1})$^{-1}$. The arrow shows the emission intensity changes upon increasing DNA concentration. Plots of [DNA]/($\varepsilon_a - \varepsilon_f$) *vs.* [DNA] for the titration complex and ligand with CT-DNA.

charged Zn(II) complex where additional interaction between the complex and phosphate rich DNA backbone may occur [49, 50]. The interaction of Zn(II) complex with DNA due to the partial intercalation of ligand in other related paper is similar with our conclusion [51, 52].

3.3.2. Fluorescence spectra. The ability of a complex to affect the intensity of EB fluorescence in the EB-DNA adduct allows determination of the affinity of the complex for DNA, whatever the binding mode may be. If a complex can displace EB from DNA, the fluorescence of the solution will be reduced due to the fact that free EB molecules are readily quenched by water [53]. For all the compounds, no emission was observed either alone or in the presence of CT-DNA in the buffer. The fluorescence quenching of DNA–bound EB by the complex and ligand are shown in figure 3. The behavior of both complex and ligand is in agreement with the Stern–Volmer equation, which provides further evidence that the complex and ligand bind to DNA. The K_{sv} values for complex and ligand are 1.64×10^4 ($R = 0.98$ for 14 points) and 1.01×10^3 (mol L^{-1})$^{-1}$ ($R = 0.99$

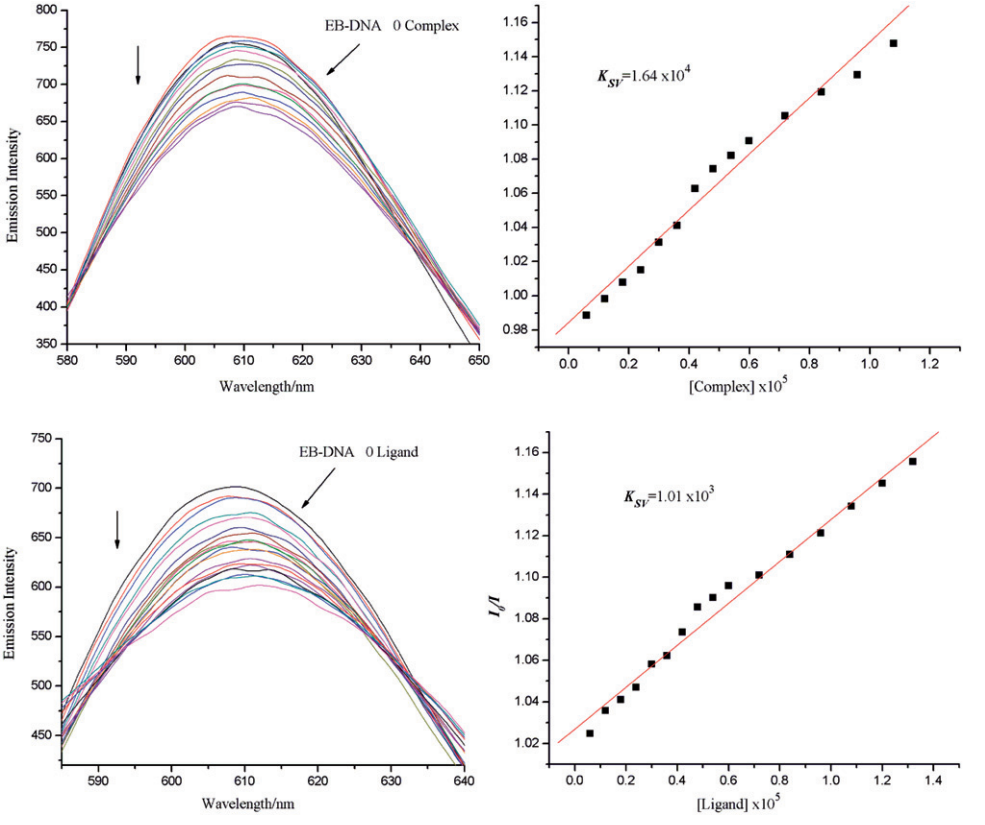

Figure 3. Emission spectra of EB bound to CT-DNA in the presence of complex and ligand; [Complex], [Ligand] = 3×10^{-5} mol L^{-1}; $\lambda_{ex} = 520$ nm. The arrows show the intensity changes upon increasing concentrations of the complex. Fluorescence quenching curves of EB bound to CT-DNA by complex and ligand.

for 16 points), respectively. The data suggest that interaction of complex with CT-DNA is stronger than ligand, consistent with the UV-Vis results [47].

3.3.3. Viscosity studies. Hydrodynamic measurements that are sensitive to DNA length changes are regarded as the least ambiguous and most critical tests of a binding model in solution in the absence of crystallographic structural data [54, 55]. For the free ligand and the complex, as increasing amounts of the compounds are added, viscosity of DNA increases steadily. The values of $(\eta/\eta_0)^{1/3}$ were plotted against [compound]/[DNA]. In classical intercalation, the DNA helix lengthens as base pairs are separated to accommodate the bound ligand, leading to increased DNA viscosity, whereas a partial, nonclassical intercalation causes a bend (or kink) in the DNA helix and so reduces its effective length and thereby its viscosity [56].

The effects of the complex and ligand on the viscosity of CT-DNA are shown in figure 4. The viscosity of CT-DNA increased steadily with increasing amounts of the compounds, providing further evidence that the complex and ligand intercalate with CT-DNA [57].

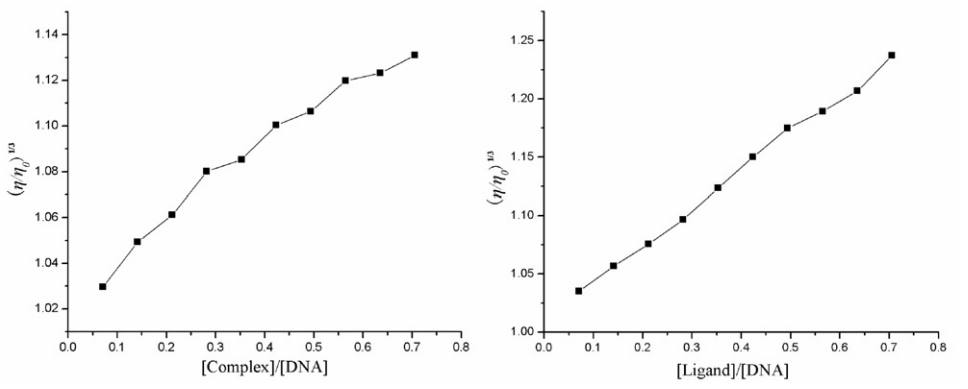

Figure 4. Effect of increasing amounts of complex and ligand on the relative viscosity of CT-DNA at 25.0 ± 0.1°C.

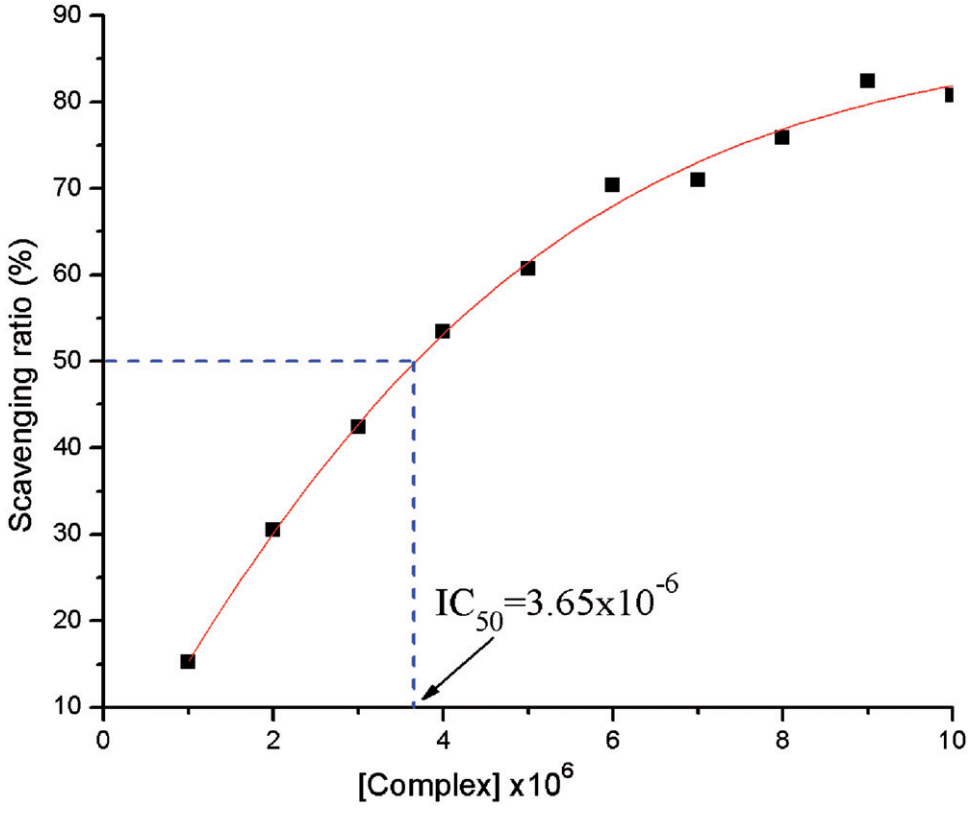

Figure 5. The inhibitory effect of complex on OH· radicals; the suppression ratio increases with increasing concentration of the test complex.

3.3.4. Antioxidant activity. We compared the abilities of the compound to scavenge hydroxyl radicals with those of the well-known natural antioxidants mannitol and vitamin C, using the same method as reported in a previous paper [58]. The 50% inhibitory concentration (IC_{50}) value of mannitol and vitamin C are 9.6×10^{-3} and 8.7×10^{-3} $(\text{mol L}^{-1})^{-1}$, respectively. According to the antioxidant experiments, the IC_{50} value of complex is 3.65×10^{-6} $(\text{mol L}^{-1})^{-1}$ (figure 5), which implies that the scavenging activity of the complex is much better than those of mannitol and vitamin C. The possible reason is that the larger conjugated metal complex can react with $HO^{\bullet}$ to form larger stable macromolecular radicals. Similar properties were reported in a related study [51]. In view of the observed IC_{50} values, the Zn(II) complex can be considered as a potential drug to eliminate hydroxyl radical.

4. Conclusion

Tris(2-(N-methyl)benzimidazylmethyl)amine (Mentb) and its Zn(II) complex have been synthesized and characterized. The binding of Zn(II) complex and ligand with CT-DNA have been studied. Photophysical and viscosity measurements indicate that the compounds interact with CT-DNA through intercalative binding. Their affinity to DNA follows the order complex > ligand, which can be attributed to charge transfer and reducing the charge density of the plane conjugate system upon coordination to the metal. The hydroxyl radical scavenging properties of the complex were also investigated, and the results show that the Zn(II) complex exhibits effective scavenging of hydroxyl radicals. The Zn(II) complex has many potential practical applications for development of nucleic acid molecular probes and new therapeutic reagents for diseases on the molecular level and warrants further *in vivo* experiments and pharmacological assays.

Supplementary material

Crystallographic data (excluding structure factors) for the structures reported in this paper have been deposited with the Cambridge Crystallographic Data Centre with reference number CCDC 859575. Copies of the data can be obtained free of charge on application to the CCDC, 12 Union Road, Cambridge CB2 1EZ, UK. Tel: +44-01223-762910; Fax: +44-01223-336033; E-mail: deposit@ccdc.cam.ac.uk or http://www.ccdc.cam.ac.uk

Acknowledgments

The authors acknowledge the financial support and grant from "Qing Lan" Talent Engineering Funds by Lanzhou Jiaotong University. The grant from "Long Yuan Qing Nian" of Gansu Province also is acknowledged.

References

[1] J. Reedijk. *Comprehensive Coordination Chemistry*, Vol. 2, Pergamon, Oxford (1987).
[2] M. Boca, R. Boca, G. Kickelbick, W. Linert, I. Svoboda. *Inorg. Chim. Acta*, **338**, 36 (2002).
[3] R. Boca, P. Baran, M. Boca, L. Dihan, H. Fuess. *Inorg. Chim. Acta*, **278**, 190 (1998).
[4] H.Y. Shrivastava, M. Kanthimathi, U.N. Balachandran. *Biochim. Biophys. Acta*, **149**, 1573 (2002).
[5] H.M.J. Hendriks, P.J.M.W.L. Birker, G.C. Verschoor, J. Reedijk. *J. Chem. Soc., Dalton Trans.*, 623 (1982).
[6] Z.X. Su, Y.Q. Wan, H.L. Wu. *Synth. React. Inorg. Met.-Org. Nano-Met. Chem.*, **35**, 553 (2005).
[7] H.L. Wu, Y.C. Gao, K.B. Yu. *Transit. Met. Chem.*, **29**, 175 (2004).
[8] H.L. Wu, W. Ying, L. Pen, Y.C. Gao, K.B. Yu. *Synth. React. Inorg. Met.-Org. Chem.*, **34**, 1019 (2004).
[9] H.L. Wu, Y.C. Gao. *J. Coord. Chem.*, **59**, 137 (2006).
[10] Y. Zhang, R. Yang, F. Liu, K. Li. *Anal. Chem.*, **76**, 7336 (2004).
[11] J. Sisko, A.J. Kassick, M. Mellinger, J.J. Filan, A. Allen, M.A. Olsen. *J. Org. Chem.*, **65**, 1516 (2000).
[12] B. Armitage. *Chem. Rev.*, **98**, 1171 (1998).
[13] W.K. Rgozelski, T.D. Tullius. *Chem. Rev.*, **98**, 1089 (1998).
[14] C. Tu, Y. Shao, N. Gan, Q. Xu, Z. Guo. *Inorg. Chem.*, **43**, 4761 (2004).
[15] M. Oivanen, S. Kuusela, H. Lonnberg. *Chem. Rev.*, **98**, 961 (1998).
[16] S.M. Hecht. *J. Nat. Prod.*, **63**, 158 (2000).
[17] J.G. Liu, B.H. Ye, H. Li, Q.X. Zhen, L.N. Ji, Y.H. Fu. *J. Inorg. Biochem.*, **76**, 265 (1999).
[18] X. Sheng, X. Guo, X.M. Lu, G.Y. Lu, Y. Shao, F. Liu, Q. Xu. *Bioconjugate Chem.*, **19**, 490 (2008).
[19] Y. Li, Z.Y. Yang, Z.C. Liao, Z.C. Han, Z.C. Liu. *Inorg. Chem. Commun.*, **13**, 1213, (2010).
[20] J. Qian, L.P. Wang, W. Gu, X. Liu, J.L. Tian, S.P. Yan. *J. Coord. Chem.*, **64**, 2480 (2011).
[21] S. Satyanaryana, J.C. Dabrowiak, J.B. Chaires. *Biochemistry*, **32**, 2573 (1993).
[22] J. Marmur. *J. Mol. Biol.*, **3**, 208 (1961).
[23] A.M. Pyle, J.P. Rehmann, R. Meshoyrer, C.V. Kumar, N.J. Turro, J.K. Barton. *J. Am. Chem. Soc.*, **111**, 3051 (1989).
[24] A. Wolf, G.H. Shimer, T. Meehan. *Biochemistry*, **26**, 6392 (1987).
[25] B.C. Baguley, M.L. Bret. *Biochemistry*, **23**, 937 (1984).
[26] J.R. Lakowicz, G. Webber. *Biochemistry*, **12**, 4161 (1973).
[27] C.P. Tan, J. Liu, L.M. Chen, S. Shi, L.N. Ji. *J. Inorg. Biochem.*, **102**, 1644 (2008).
[28] C.C. Winterbourn. *Biochem. J.*, **198**, 125 (1981).
[29] C.C. Winterbourn. *Biochem. J.*, **182**, 625 (1979).
[30] Z.Y. Guo, R.E. Xing, S. Liu, H.H. Yu, P.B. Wang, C.P. Li. *Bioorg. Med. Chem. Lett.*, **15**, 4600 (2005).
[31] H.M.J. Hendriks, P.J.M.W.L. Birker, G.C. Verschoor, J. Reedijk. *J. Chem. Soc., Dalton Trans.*, 623 (1982).
[32] Bruker. *Smart Saint and Sadabs*, Bruker AXS Inc., Madison, WI (2000).
[33] G.M. Sheldrick. *SHELXTL*, Siemens Analytical X-Ray Instruments Inc., Madison, WI (1996).
[34] C.Y. Su, B.S. Kang, C.X. Du, Q.C. Yang, T.C.W. Mak. *Inorg. Chem.*, **39**, 4843 (2000).
[35] T.J. Lane, I. Nakagawa, J.L. Walter, A.J. Kandathil. *Inorg. Chem.*, **1**, 267 (1962).
[36] M. McKee, M. Zvagulis, C.A. Reed. *Inorg. Chem.*, **24**, 2914 (1985).
[37] K. Nakamoto. *Infrared and Raman Spectra of Inorganic and Coordination Compounds*, 3rd Edn, pp. 200–320, John Wiley and Sons, New York (1978).
[38] J. Catterick, P. Thornton. *Adv. Inorg. Chem.*, **20**, 291 (1977).
[39] S. Musumeci, E. Rizzarelli, S. Sammartano, A. Seminaba. *Z. Anorg. Allg. Chem.*, **433**, 297 (1977).
[40] H.L. Wu, J.G. Liu, P. Liu, W.B. Lv, B. Qi, X.K. Ma. *J. Coord. Chem.*, **61**, 1027 (2008).
[41] Z.X. Su, Y.Q. Wan, H.L. Wu. *Synth. React. Inorg. Met.-Org. Nano-Met. Chem.*, **35**, 553 (2005).
[42] S. Youngme, J. Phatchimkun, U. Sukangpanya, C. Pakawatchai, N. Chaichit, P. Kongsaeree, J. Krzystek, B. Murphy. *Polyhedron*, **26**, 871 (2007).
[43] H. Li, X.Y. Le, D.W. Pang, H. Deng, Z.H. Xu, Z.H. Lin. *J. Inorg. Biochem.*, **99**, 2240 (2005).
[44] V.G. Vaidyanathan, B.U. Nair. *Eur. J. Inorg. Chem.*, **19**, 3633 (2003).
[45] V.G. Vaidyanathan, B.U. Nair. *Eur. J. Inorg. Chem.*, **9**, 1840 (2004).
[46] J. Liu, T.X. Zhang, L.N. Ji. *J. Inorg. Biochem.*, **91**, 269 (2002).
[47] H.L. Wu, K. Li, T. Sun, F. Kou, F. Jia, J.K. Yuan, B. Liu, B.L. Qi. *Transit. Met. Chem.*, **36**, 21 (2011).
[48] H.L. Wu, F. Kou, F. Jia, B. Liu, J.K. Yuan, Y. Bai. *J. Photochem. Photobiol. B*, **105**, 190 (2011).
[49] S. Yellappa, J. Seetharamappa, L.M. Rogers, R. Chitta, R.P. Singhal, F. D'Souza. *Bioconjugate Chem.*, **17**, 1418 (2006).
[50] M. Shakir, M. Azam, M.-F. Ullah, S.-M. Hadi. *J. Photochem. Photobiol. B*, **104**, 449 (2011).
[51] P. Maiti, A. Khan, T. Chattopadhyay, S. Das, K. Manna, D. Bose, S. Dey, E. Zangrando, D. Das. *J. Coord. Chem.*, **64**, 3817 (2011).
[52] A.K. Asatkar, S. Nair, V.K. Verma, C.S. Verma, T.A. Jain, R. Singh, S.K. Gupta, R.J. Butcher. *J. Coord. Chem.*, **65**, 28 (2012).
[53] J.B. LePecq, C. Paoletti. *J. Mol. Biol.*, **27**, 87 (1967).

[54] S. Mahadevan, M. Palaniandavar. *Inorg. Chem.*, **37**, 693 (1998).
[55] A.B. Tossi, J.M. Kelly. *Photochem. Photobiol.*, **49**, 545 (1989).
[56] S. Satyanarayana, J.C. Dabrowiak, J.B. Chaires. *Biochemistry*, **32**, 2573 (1993).
[57] S. Satyanarayana, J.C. Dabrowiak, J.B. Chaires. *Biochemistry*, **31**, 9319 (1992).
[58] T.R. Li, Z.Y. Yang, B.D. Wang, D.D. Qin. *Eur. J. Med. Chem.*, **43**, 1688 (2008).